

Article

Hydrogels Obtained *via* γ -Irradiation Based on Poly(Acrylic Acid) and Its Copolymers with 2-Hydroxyethyl Methacrylate

Marin Micutz ¹, Rodica Mihaela Lungu ², Viorel Circu ³, Monica Ilis ³ and Teodora Staicu ^{1,*}

¹ Department of Physical Chemistry, University of Bucharest, 4-12 Regina Elisabeta Blvd., 030018 Bucharest, Romania; micutz@gw-chimie.math.unibuc.ro

² Scientific Research Center for CBRN Defense and Ecology, 225 Oltenitei st., 041309 Bucharest, Romania; rodica.lungu@nbce.ro

³ Department of Inorganic Chemistry, University of Bucharest, 23 Dumbrova Rosie st., 020464 Bucharest, Romania; viorel.circu@chimie.unibuc.ro (V.C.); monica.ilis@chimie.unibuc.ro (M.I.)

* Correspondence: teos@gw-chimie.math.unibuc.ro

Received: 19 June 2020; Accepted: 17 July 2020; Published: 19 July 2020



Abstract: Hydrogels containing both carboxyl and hydroxyl functional groups have been prepared by γ -irradiation of either aqueous solutions of acrylic acid (AA) and mixtures of AA and 2-hydroxyethyl methacrylate (HEMA) in different ratios, or aqueous solutions of poly(AA), PAA, and poly(AA-co-HEMA) obtained via solution polymerization. A higher absorbed dose is required in order to prepare hydrogels from monomer solutions, compared with those from polymer solutions. The range for the absorbed doses was chosen so that the probability of crosslinking reactions is higher than that of degradation ones. As the radiation energy deposited in a sample increases, the equilibrium swelling degree and the average molar mass between crosslinks diminishes. Chemical transformations induced by radiation were investigated by means of FTIR spectroscopy and thermal analysis of polymers before and after irradiation. For all these systems, the formation of a three-dimensional network enhances the glass transition temperature and thermal stability, but a further increase in the crosslinking degree may have the reverse effect on the glass transition temperature. Depending on the preparation protocol and/or hydrogel composition, superabsorbent materials that can bind different compounds throughout side functional groups may be obtained.

Keywords: hydrogels; γ -irradiation; swelling; thermal behavior; poly(acrylic-acid)

1. Introduction

Hydrogels are three-dimensional networks of hydrophilic polymers capable of absorbing important quantities of water. The amount of water uptake may widely vary, starting from tens of grams per 1 g of dry gel to thousands of grams. By general definition, superabsorbent hydrogels are those that can retain an amount of liquid greater than 100 times its own weight in dry state. Both physically and chemically crosslinked hydrogels have been intensively studied in the last 50 years. As practically any water-soluble polymer can be turned into a hydrogel, the number of chemical compositions is vast and practical applications continue to grow. Starting from commercially available products such as diapers or contact lenses, due to their unique physical properties, hydrogels rapidly emerge into fields like tissue engineering [1–5], or other biomedical applications, including drug-delivery [6,7], but also in the field of detectors, actuators, etc., [8–13].

By their ability to respond to external stimuli such as pH, temperature, light, solvent, ionic strength, concentration [14–18], hydrogels, more than any other biomaterials, can mimic different living tissues [2,19,20]. Acidic polymers, like poly(acrylic acid), PAA, or poly(methacrylic acid), PMA, which

can form pH-responsive hydrogels are often grafted on different biopolymers [21] or copolymerized in the presence of other monomers or polymers [22] to obtain functional materials. At the same time, poly(2-hydroxyethyl methacrylate), PHEMA, employed either as homopolymer or copolymer, is another valuable candidate to be used for obtaining hydrogels. As a result of its peculiarities (good chemical and thermal stability, transparent to visible light, inert to biological environment or an excellent cytocompatibility) [23–25], such a hydrophilic component could be successfully utilized and chemically incorporated in tuning the swelling capacity of PAA-based hydrogels.

The crosslinking of different systems using high energy radiation represents an alternative to chemical crosslinkers that may be many times toxic, especially when pharmaceutical materials were intended to be obtained. Thus, photoinduced crosslinking using UV and near-UV radiation [26], electron beam or γ radiation [27–30] applied to a great variety of solid polymers or aqueous solutions of homopolymers, copolymers, or even monomers can lead to hydrogels with specific applications. While irradiation of solid polymers can be disadvantageous in terms of sample homogeneity and the requirement of high absorbed dose, aqueous solutions of polymers or monomers are successfully used in preparing hydrogels that are free of impurities and sterilized at the same time.

In this paper we focused on preparing copolymers of acrylic acid and 2-hydroxyethyl methacrylate via solution polymerization and subsequently crosslinked them by γ irradiation to produce functional hydrogels with adjustable loading capacity. The presence of both carboxyl and hydroxyl groups in the same macromolecular chain favors intermolecular interactions leading to more thermally stable compounds compared to the corresponding homopolymers. The molar ratio between monomers was chosen so that the resultant copolymers remain soluble in water at a pH as low as 3. Aqueous solutions of the copolymers were subjected to γ irradiation to prepare hydrogels with different crosslinking densities. For comparison, mixtures of the same composition monomers in aqueous solutions were also subjected to γ irradiation and the hydrogels so obtained were studied in terms of their swelling equilibrium. Depending on the preparation protocol and/or hydrogel composition superabsorbent materials that can bind different compounds throughout side functional groups may be obtained.

2. Materials and Methods

2.1. Materials

Acrylic acid ($\geq 99\%$, Fluka, Buchs, Germany), AA, and 2-hydroxyethyl methacrylate ($\geq 99\%$, Fluka, Buchs, Germany), HEMA, as monomers, and potassium persulfate ($+99\%$, Sigma-Aldrich, Steinheim, Germany), KPS, as initiator were used as received.

2.2. Solution Polymerization

PAA and copolymers of AA and HEMA with different molar ratios between comonomers were prepared via solution polymerization using KPS as initiator. Three AA/HEMA molar ratios were considered: 18/1, 9/1, and 3/1 denoted by **PAH18**, **PAH9**, and **PAH3**, respectively. The final concentration for the polymer solution was about 10 wt.% to avoid copolymer precipitation, especially at higher content of HEMA. The monomer or mixture of monomers was placed into a round bottom reactor equipped with a mechanical stirrer, refrigerant, and an inlet for argon feed. The reactor temperature was maintained constant by using a water bath. After bubbling argon for about 30 min for air removal, the temperature was raised to 70 °C and 0.037 M KPS water solution was injected under mechanical stirring to initiate polymerization. The reaction was carried out for 3 h at the same constant temperature. For **PAH3** system, the obtained copolymer was no longer soluble in water and precipitates.

After cooling the polymer solutions, the unreacted monomers and initiator were removed by dialysis against distilled water, using dialysis tubing with a molecular mass cut-off of 14,000 Da. The final solution concentrations were determined gravimetrically. Three samples from each polymer solution were weighed and placed in an oven at a temperature of 90 °C for water evaporation. After the

samples reached a constant mass, their concentrations were calculated, and the final value was the mean of the three measurements.

Samples with concentration of approximately 0.25% were prepared by dilution with distilled water and then titrated with a strong base, NaOH. The acid-base titrations were monitored potentiometrically using a pH glass electrode connected to a multi-parameter analyzer Consort C861.

Intrinsic viscosities, $[\eta]$, were determined from capillary viscosity measurements, at 25 ± 0.1 °C, using an Ubbelohde viscometer. The particular concentrations of the samples prepared by dilution were chosen to give specific viscosities below 0.7, all the solutions being adjusted to pH 3 using HCl 1N.

2.3. Hydrogel Preparation

Aqueous solutions (2 wt.%) of monomers in appropriate ratios were placed in 2 mL plastic ampoules. The prepared polymer solutions were diluted to a concentration of 2 wt.% and the pH was adjusted to 3 and placed into the same kind of tubes. Sample irradiation was carried out in air at room temperature using a GAMMATOR irradiator containing a ^{137}Cs source with a dose rate of 0.4 kGy/h.

2.4. Swelling Equilibrium

To remove soluble radiolysis products immediately after irradiation, the prepared hydrogels were rinsed with distilled water several times per day for two weeks until reaching a constant weight for the dried samples. The gel fraction, g_f , was calculated as the ratio between the xerogel mass after removing soluble components and the initial polymer weight in the sample, before irradiation.

After washing and drying, the xerogels were left to reswell in distilled water at room temperature. The swollen hydrogels were withdrawn from water, wiped with filter paper to remove excess surface water, and weighed. Equilibrium was reached when the hydrogels attained a constant mass. Equilibrium degree of swelling, SD_{eq} , was calculated as:

$$SD_{eq} = \frac{m_s - m_d}{m_d} \quad (1)$$

where m_s is the weight of the hydrogel at equilibrium swelling and m_d is the weight of the dry gel. The swelling procedure was performed for three samples from each xerogel and the mean values were considered.

The swelling data were used to evaluate the average mass between crosslinks (M_c) and the crosslinking degree (d_c). The first structural parameter was calculated using Flory–Rehner equation [31]:

$$M_c = -\frac{\rho_x V_w \phi_2^{1/3}}{\ln(1 - \phi_2) + \phi_2 + \chi \phi_2^2} \quad (2)$$

where ρ_x is the xerogel density, V_w —the molar volume of water, ϕ_2 —the polymer volume fraction, and χ —the polymer-solvent interaction parameter. The values for χ were calculated by the following relationship [32]:

$$\chi = \frac{\ln(1 - \phi_2) + \phi_2}{\phi_2^2} \quad (3)$$

with ϕ_2 given by:

$$\phi_2 = \frac{1}{1 + \frac{\rho_x}{\rho_w} SD_{eq}} \quad (4)$$

where ρ_w is the density of water.

The density of the xerogels was picnometrically determined using toluene as a nonsolvent ($\rho_{\text{toluene}} = 0.8768$ g/cm³). The measurements were done in triplicate at 20 ± 0.1 °C.

In the case of an ideal tetrafunctional network, the number of crosslinking points in 1 mL of polymer, i.e., crosslinking degree, can be evaluated using the equation below [30]:

$$d_c = \frac{\rho_x}{2M_c} \quad (5)$$

2.5. FTIR Spectroscopy

The ATR FTIR spectral measurements were performed using a FTIR 6300 Jasco equipped with a single reflection diamond ATR crystal with incidence angle of 30°. Absorption spectra (each of them being an average of 16 scans) were recorded in the wavenumber range of 4000–600 cm⁻¹ with 4 cm⁻¹ resolution.

2.6. Differential Scanning Calorimetry (DSC)

Differential scanning calorimetry (DSC) investigation was performed for dried samples using a Diamond DSC Perkin-Elmer with nitrogen purge at a heating rate of 10 K/min between 20 and 180 °C. Glass transition temperature (T_g) was considered the inflection point on the dependence of heat flow vs. temperature, obtained during the second heating.

2.7. Thermogravimetric Analysis (TGA)

Thermal stability of all samples was studied by employing Thermogravimetric Analyzer Q50 (TA Instruments) under nitrogen atmosphere, from room temperature to 550 °C with a heating rate of 10 K/min.

The pH and conductometric titrations, capillary viscometry, swelling, DSC and TG measurements were performed in triplicate. Excepting the equilibrium swelling investigations, where relative standard deviation (RSD) was less than 15%, all the other above-mentioned determinations led to experimental data with RSD values lower than 2%.

3. Results and Discussion

3.1. Solution Polymerization

The polymer solutions resulted after removing the low molecular mass compounds had final concentrations around 5 wt.% and pH about 2.5–3.

The number of carboxyl groups for PAA and its copolymers with HEMA was determined by pH and conductometric titration with NaOH solution (4.76×10^{-2} M). Typical titration curves for weak acids were obtained, as can be seen in Figure 1. For a weak acid such as PAA or its copolymers, the conductometric titration was more suitable for identifying the equivalence point (Figure 1b), while the pH titration curves were used to find out the apparent acidity exponent of polymer $pK_{a,app}$ (Figure 1a). Literature data indicated a pK_a of 4.25 for AA, while values starting from 4.5 to 6.8 were reported for PAA [33–37]. Nevertheless, covalently binding of the AA residues within the polymer chain negatively affected the degree of dissociation due to the repulsive interactions between the neighboring carboxylate groups. Indeed, a $pK_{a,app}$ of 6.36 was obtained for PAA.

For PAA the number of moles of carboxyl groups determined from the volume of NaOH solution used to attain the equivalence point (1.33×10^{-2} mole/g of polymer) was very close to that theoretically expected (1.39×10^{-2} mole/g of polymer). For copolymers, the differences between the two quantities (experimentally and theoretically obtained) could offer some insights about the ratio between AA and HEMA units in copolymer backbone.

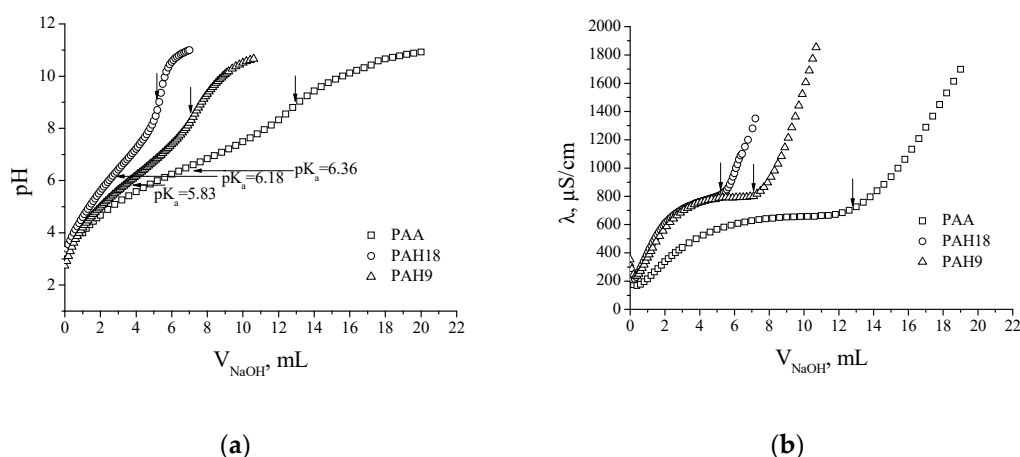


Figure 1. Curves of (a) pH and (b) conductometric titration for 0.25% polymer solutions.

It can be easily observed in Figure 1a,b that the volume of NaOH solution used to neutralize all carboxyl groups was much lower for copolymers compared with PAA in spite of the fact that samples having the same concentration of polymer were used. Thus, the number of carboxyl groups determined from titration curves represented only 60% from the theoretical number calculated for PAH9 and 45% for PAH18. Even though the method was not very accurate, it could be concluded that the molar ratio between AA and HEMA units in copolymer was smaller than in the initial mixture of monomers. Thus, although the ratio between AA and HEMA in the initial monomer mixture was very high for both copolymers (18 and 9, respectively), due to the very uneven reactivity ratios of these monomers, the copolymer composition was different, with much smaller ratios between the same monomer units. The values reported for reactivity ratios being 4.382 for HEMA and 0.131 for AA [38], it was expected that the copolymer would be enriched in HEMA units when compared with the substrate. This was proved also by the fact that for a molar ratio of AA/HEMA equal to 3/1, the resulting copolymer was insoluble in water at low pH. Such behavior was due to a larger content of HEMA monomer units than AA ones in PAH3 which were responsible for reducing the water solubility of this copolymer. On the other hand, based on the product value of the two reactivity ratios (0.574), the copolymerization of the discussed comonomer mixtures might be considered as nonideal, being placed almost symmetrically between the alternating and ideal type of radical copolymerization. This conclusion is in good agreement with that arising from the Q-e scheme. Even though the reactivity ratios calculated according to this empirical model (1.460 for HEMA and 0.355 for AA) [39] were significantly different from the same quantities experimentally determined, the product of them (0.518) practically indicated a quite similar nonideal kind of copolymerization.

Copolymers PAH18 and PAH9 are stronger acids than PAA, as can be seen in Figure 1. As the number of HEMA monomer units increased in the copolymer, the distance between carboxyl groups increased, favoring their dissociation. As a consequence, $pK_{a,app}$ was expected to be lower for copolymer PAH9. Indeed, these values experimentally obtained were 6.18 for PAH18 and 5.83 for PAH9.

By plotting specific viscosities, η_{sp} , on solution concentration, c (see Figure 2a), one can notice that all polymers behave like a neutral polymer, i.e., $\eta_{sp} \sim c^{1.0}$, for the chosen concentration range [40].

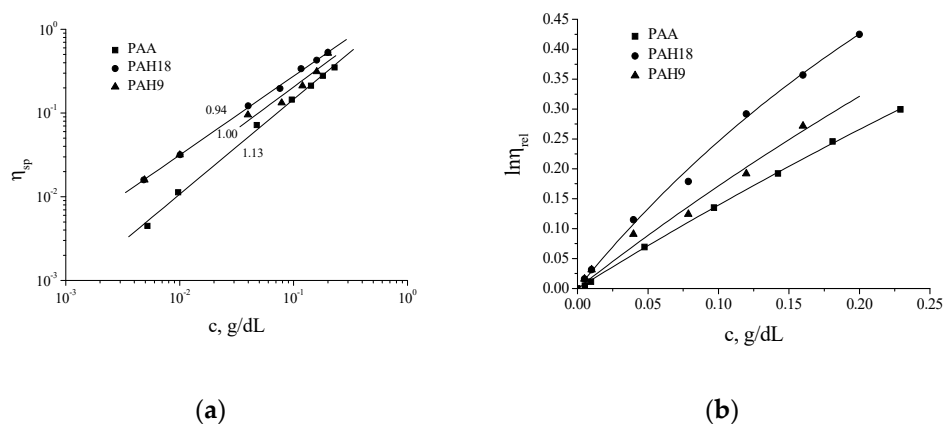


Figure 2. (a) Specific viscosity as a function of polymer concentration (the numbers indicate the values of the slopes), and (b) logarithm of relative viscosity vs. polymer concentration.

Accordingly, intrinsic viscosities, $[\eta]$, were evaluated by using a simplified Wolf equation applicable to neutral polymers [41]:

$$\ln \eta_{rel} = \frac{c[\eta]}{1 + Bc[\eta]} \quad (6)$$

where η_{rel} is the relative viscosity, and B a fitting parameter. Based on experimental data from Figure 2b fitted to Equation (6), the following values for $[\eta]$ were determined: 1.47, 2.92, and 1.84 dL/g for PAA, PAH18, and PAH9, respectively. Consequently, the overlapping concentration, c^* , for the same polymers, calculated as the inverse of $[\eta]$ [40], are 0.68, 0.34, and 0.54%, respectively.

3.2. Hydrogel Preparation

Hydrogels prepared by γ -irradiation of aqueous solutions of hydrophilic polymers or water soluble monomers present a series of advantages over chemical crosslinking hydrogels: easy process control, fortunately combining hydrogel formation with sterilization in one step, the lack of any initiators, catalysts or crosslinkers that are possibly toxic or difficult to remove, no higher temperatures needed, no wastes, etc. Moreover, unreacted monomers can be easily removed by washing with water. However, irradiation of monomer mixtures implies first the initiation of the polymerization reaction followed by crosslinking. In the case of monomers like AA and HEMA, the resulting hydrogels were not homogenous, in spite of the fairly uniform distribution of the irradiation field. Thus, poly(HEMA) chains that were not soluble in water tended to locally separate and even if eventual crosslinking with PAA chains were to take place, the resulted hydrogel would no longer be homogenous in its entire mass. This assertion was sustained not only by visual observation of the hydrogel, but also by DSC measurements that indicated two glass transitions (not shown). This last aspect may be an indication of the existence of either a mixture of two homopolymers (PAA + PHEMA) or some species of block copolymer (PAA-b-PHEMA) or a mixture of the two types of macromolecular components. However, due to the huge difference between the reactivity ratios of the two monomers, the nonhomogeneous hydrogel most likely consisted of individually synthesized PAA and PHEMA chemically linked together as a result of the irradiation process. Consequently, hydrogels prepared by this method were not further characterized by swelling equilibrium degree, FTIR or TGA. Moreover, at low absorbed doses (below 30 kGy), hydrogels were obtained only for AA solutions, while for AA/HEMA solutions the gelation dose was higher than 30 kGy, with no gel formation at lower doses.

Based on capillary viscometry data, all polymer solutions having concentrations of about 2 wt.% and pH 3 are well above the overlapping concentration, thus intermolecular crosslinks are favored. At the same time, the volume fractions of polymers in these solutions are small enough and superabsorbent hydrogels can form. At such a low pH, hydrogen bonding between the functional groups of copolymers is also favored. Besides, as the polymer chains are already synthesized,

the crosslinking efficiency induced by γ -rays is substantially improved and hydrogels can be formed even at small absorbed doses in spite of low polymer concentration.

The interaction of high-energy radiation with polymer solutions induces various chemical transformations both in polymer chains and water. For solutions with low or moderate concentrations, the direct action of radiation on the macromolecular backbone is less important compared with the indirect one, i.e., reactions of the polymer with the radiolysis intermediates generated by water. Hydroxyl radicals have been shown to be the main responsible species for radiochemical transformations induced by water onto the polymer chains. They abstract hydrogen atoms from macromolecules, forming macroradicals [42]. Intermolecular crosslinking appears either when two macroradicals with high enough mobility are able to react to each other, or when macroradicals could be involved in chain transfer reactions to polymer molecules.

3.3. Swelling Equilibrium

The degree of crosslinking of the obtained hydrogels was assessed by swelling equilibrium measurements. As expected, as the absorbed dose increased, both the swelling equilibrium and average molecular mass between crosslinks decreased, which was equivalent to saying that the degree of crosslinking rose at a higher absorbed dose.

Although the density of polymers was enhanced after crosslinking, the influence of the absorbed dose on density was not significant. Thus, all irradiated polymers have densities in the range of 1.51–1.56 g/cm³, being higher than those of the un-crosslinked PAA (1.20 g/cm³), PAH18 (1.21 g/cm³), and PAH9 (1.18 g/cm³). Consequently, variation of the parameters M_c , d_c or ϕ_2 with the adsorbed dose may entirely be correlated with the equilibrium degree of swelling.

Nevertheless, the gel fraction for samples PAA, PAH18, and PAH9 was above 0.95, which indicated that the absorbed energy was not excessively high to damage the polymer chains instead of making desirable crosslinking between them.

The influence of increasing absorbed dose on structural parameters of the prepared hydrogels is shown in Table 1.

Table 1. Effect of absorbed dose on SD_{eq} , M_c , and d_c .

Sample	D, kGy	SD_{eq} , g/g	$M_c \times 10^{-5}$, g/mol	d_c , mol/m ³
PAA	30	112	1.56	4.78
	40	117	1.48	5.07
	50	58	0.48	16.36
PAH18	30	151	2.25	3.33
	40	116	1.45	5.17
	50	58	0.45	17.47
PAH9	30	164	2.58	2.91
	40	115	1.44	5.22
	50	88	1.00	8.03
AA	30	547	10.67	0.56
	50	96	1.07	7.07
	70	92	1.02	7.47
AA/HEMA 18/1	30	-	-	-
	50	268	6.08	1.25
	70	107	1.30	5.83
AA/HEMA 9/1	30	-	-	-
	50	186	3.31	2.30
	70	147	2.16	3.48

The data from Table 1 show that, for a certain absorbed dose, when aqueous monomer solutions were irradiated instead of polymer solutions, the resulting hydrogels had lower crosslinking degrees. Also comparing the degree of swelling and the average mass between crosslinks obtained for the

same absorbed dose, one can notice a significant increase in both parameters in the case of monomer solutions. This was probably because a fraction of hydroxyl radicals generated by irradiation was consumed to start the polymerization reaction.

3.4. FTIR Measurements

To identify the radiochemical transformations of polymers, FTIR spectra of the systems in dry state were recorded. In Figure 3, FTIR spectra for PAA before and after irradiation are plotted. The absorption bands for the non-irradiated polymer are ascribed as follows: OH stretching—a broad band around 3300 cm^{-1} , CH and CH_2 stretching at $2960\text{--}2880\text{ cm}^{-1}$, C = O stretching—an intense band at 1696 cm^{-1} , CH_2 bending at 1450 cm^{-1} , C-O-H bending at 1418 cm^{-1} , C-O stretching at 1236 and 1164 cm^{-1} . The two vibrations for C-O stretching appeared due to involvement of some acid groups in the formation of hydrogen bonds, which lowered the stretching frequency for such groups. For the same reason, the prominent band corresponding to C = O stretching had a lower wavenumber than $1710\text{--}1700\text{ cm}^{-1}$ which was usually obtained for carboxylic acids. The lack of any peak around $1565\text{--}1542\text{ cm}^{-1}$ that corresponded to asymmetric stretching of COO^- proved that almost all functional groups of PAA existed in the nonionized form.

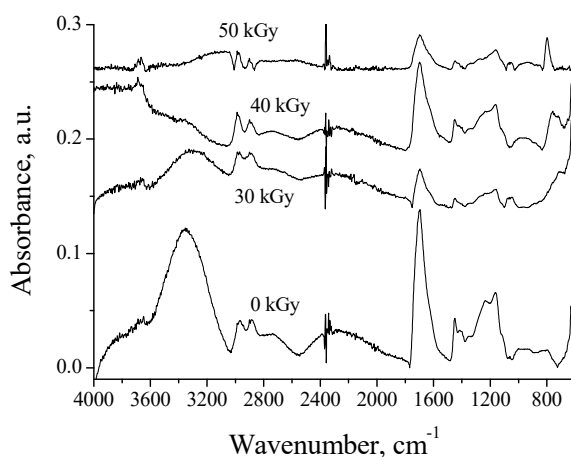


Figure 3. FTIR spectra for poly(acrylic acid) (PAA) before and after irradiation.

After irradiation, some changes in the FTIR spectra occurred. Thus, OH stretching became less visible and eventually disappeared, and the shape of the two peaks assigned to C-O stretching vibrations in carboxyl group changed. Thus, due to a certain degree of decarboxylation γ -radiation induced, both peaks located on 1236 and 1164 cm^{-1} weakened, which indicated that carboxyl groups were still present and engaged in hydrogen bonding even after irradiation. Nevertheless, a part of the functional groups attached to the monomer units were destroyed or involved in the crosslinks formed during irradiation. As a consequence, ketone and ester groups could appear, although they were difficult to identify when carboxyl groups were also present. Another important change could be observed in the region of C-O-H bending (1418 cm^{-1}). This peak also became less visible due to an easy subtraction of hydrogen.

The two copolymers, PAH18 and PAH9, have very similar FTIR spectra. Thus, in Figure 4, for better clarity, only the un-crosslinked PAH18 spectrum is presented, together with the spectra of both copolymers after irradiation at specified absorption doses. For un-crosslinked copolymers, the IR spectra were very much like the IR spectrum of PAA: broad band around 3300 cm^{-1} for OH stretching, overlapping it with CH stretching at 2960 cm^{-1} , strong peak at 1705 cm^{-1} (C = O stretching), CH_2 and OH bending at 1454 and 1413 cm^{-1} , respectively, and C-O stretching at 1260 and 1169 cm^{-1} . The two new bands at 1100 and 1020 cm^{-1} could be assigned to the stretching vibrations associated to C-O bonds in ester and alcohol moieties.

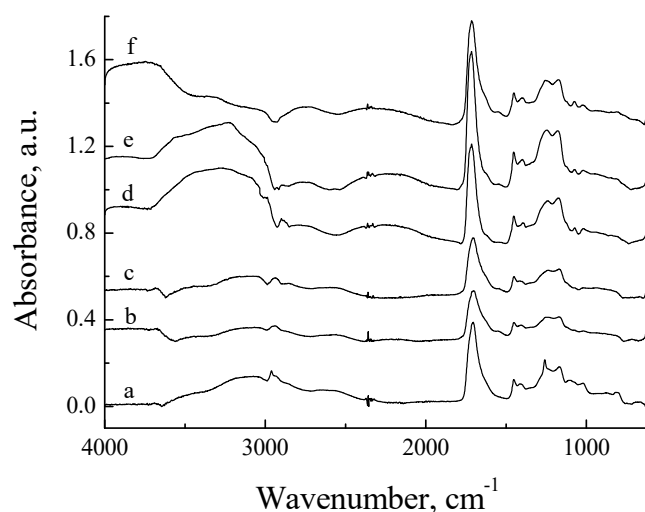


Figure 4. FTIR spectra for (a) **PAH18**; (b) **PAH18** after absorption of 40 kGy and (c) 50 kGy; (d) **PAH9** after absorption of 30 kGy, (e) 40 kGy, and (f) 50 kGy.

After irradiation of **PAH18**, the peaks located at 1100 and 1020 cm^{-1} could no longer be observed, which proved that large fractions of these side functional groups totally transformed/disappeared under the action of γ -rays. For copolymer **PAH9**, that had more HEMA units in the backbone, the peaks corresponding to ester and alcohol bonds were still present. The same conclusion could be drawn for the peak corresponding to OH bending (1413 cm^{-1}).

3.5. DSC Measurements

Molecular modifications induced by radiation were further investigated by DSC. The associated thermograms plotted in Figure 5 for the samples in dry state also provided general information about the copolymerization reaction. That a single T_g was detected for both synthesized copolymers mainly suggested the statistical character of the copolymer microstructure on molecular scale, despite very different reactivity ratios of comonomers.

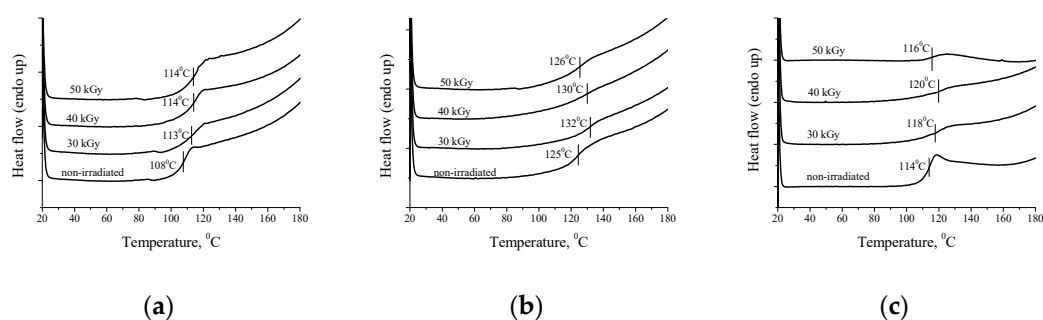


Figure 5. DSC curves for (a) **PAA**; (b) **PAH18**; (c) **PAH9**.

T_g for **PAA** was approximately 108 $^{\circ}\text{C}$ (see Figure 5a), while its copolymers with HEMA had higher glass transition temperatures (125 $^{\circ}\text{C}$ for **PAH18**, and 114 $^{\circ}\text{C}$ for **PAH9**). This is a little unusual considering that T_g of poly(HEMA) is about 100 $^{\circ}\text{C}$ [43]. According to the Fox equation, the two copolymers should exhibit a lower glass transition temperature than **PAA**. However, a positive deviation from the Fox equation indicates some attractive intermolecular interactions between polymer chains. Moreover, T_g for **PAH18** is significantly higher than T_g for **PAH9** and this fact cannot be explained by the different molar ratio between monomers in the initial substrate, but by a different molar ratio of monomer units in copolymer, mainly enriched in HEMA units.

After irradiation, the glass transition temperature of all polymers increased. However, while for PAA a further increase in the absorbed dose maintained the T_g almost unchanged, for copolymers the transition temperature diminished. This effect could be observed for PAH9 after absorption of 50 kGy and for PAH18 samples irradiated with 40 and 50 kGy. Thus, in spite of an increased crosslinking degree (see Table 1), T_g lowered, but nevertheless it remained higher than T_g of un-crosslinked polymers. This could be a direct consequence of removing some functional groups by irradiation to such an extent that the intermolecular interactions diminished. Because the mass between crosslinks was still high, even if the resulting network had more chemical crosslinking points at a higher absorbed dose, the number of intra or intermolecular interactions became smaller, allowing some parts of the polymer chains to move more freely between the neighboring two crosslinkages. Accordingly, a schematic representation of hydrogel formation by irradiation was proposed and displayed in Figure 6.

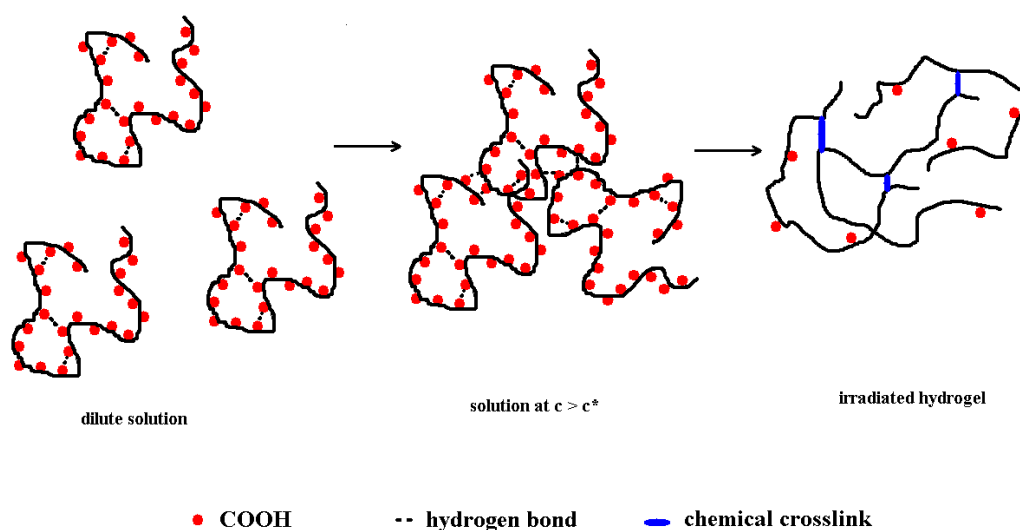


Figure 6. Schematic representation of hydrogel formation by γ -irradiation.

Indeed, increasing the absorbed dose to 70 kGy for a 2 wt.% PAA aqueous solution (results not shown), M_c became 3512 g/mol, corresponding to a crosslink density of 142 mol/m³, while the glass transition appeared at 120 °C. However, it is noteworthy that increasing the energy transferred to a polymer mass may significantly potentiate the possibility of scission of main chains as well, so the degradation reactions may occur more frequently than crosslinking ones. Consequently, the gel fraction for this particular sample of PAA was only 0.88.

3.6. TG Analysis

Thermal degradation of the synthesized polymers and the corresponding xerogels were studied by thermogravimetry. For the un-crosslinked polymers, the degradation process took place in three generally well-defined steps for PAA and four steps for PAH18 and PAH9. Thus, according to some experimental data reported elsewhere on PAA [44–47], the three steps were ascribed to water loss, 5%, (up to 185 °C), the reaction between functional groups with anhydride formation and also decarboxylation, about 35% weight loss (range 220–290 °C), and finally main chain degradation and depolymerization, 45% weight loss (above 325 °C). Because PHEMA generally decomposes with temperature in a single step [23,24,48], the analysis of thermal behavior of an AA-HEMA copolymer was much simplified. Thus, for both copolymers, the presence of HEMA units led to a new degradation step assigned to esterification reactions between functional groups. For PAH18, this new step of weight loss could be identified on the first derivative thermogravimetric (DTG) curve as a broad pick (with an onset temperature of 180 °C and the temperature at maximum reaction rate of 216 °C) partially overlapped with the sharp pick assigned to decarboxylation/anhydride formation within PAA

sequences. A similar situation was observed for **PAH9** on DTG trace, but with a much lower onset temperature of 145 °C and a temperature of maximum reaction rate of 181 °C. The difference of 35 °C between the two pick temperatures (on DTG curves) is somewhat surprising and deserves further investigation, even though we suspect that a higher proportion of hydroxyl groups as in **PAH9** means more possible hydrogen bonds established with carboxyl groups and favorable to inter/intramolecular esterification. On the other hand, increasing the number of HEMA units in the copolymers raised the temperature at which 50% of the sample was still present, T_{50} , which was higher for **PAH18** and **PAH9** (382 and 388 °C, respectively, when compared to 371 °C for **PAA**). As the thermal degradation was performed in nitrogen atmosphere, some residue, around 10–15%, was detected at the end of the thermal treatment.

Irradiation of **PAA** practically did not alter at all the onset temperature corresponding to the reaction of functional groups (even though the temperature at maximum reaction rate rose by a few degrees Celsius), while the associated weight loss decreased just a little bit (31%). At the same time, the degradation reactions started at a temperature higher than that for the non-irradiated **PAA** by ca. 14 °C (see Figure 7). Overall, the absorbed dose in the studied range did not have a significant influence on the thermal stability of the polymers.

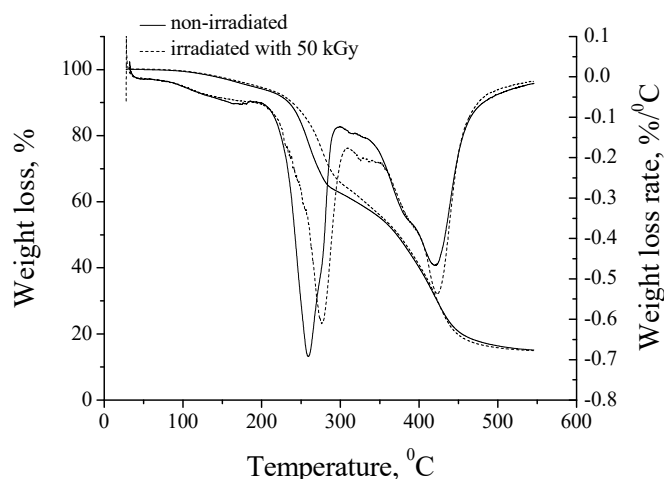


Figure 7. TG curves for **PAA** before and after irradiation.

Irradiation of both copolymers induced more significant changes than in the case of **PAA** (see Figure 8). Thus, the step corresponding to the esterification reaction was no longer visible after diminishing the number of the functional groups as a result of irradiation. Only one step of weight loss corresponding to both decarboxylation and reaction between the remaining functional groups was detected. At the same time, the weight loss corresponding to the reaction between functional groups became smaller as the irradiation dose increased, while the onset temperature increased as well. In other words, such a modified copolymer containing fewer carboxyl and hydroxyl groups, which are most likely located far from each other along the macromolecular backbone, is expected to maintain its integrity better at a certain temperature in the range of 230–350 °C.

The absorbed dose also had a significant influence (more important for **PAH9**) on the depolymerization and chain degradation step, unlike the case of **PAA**.

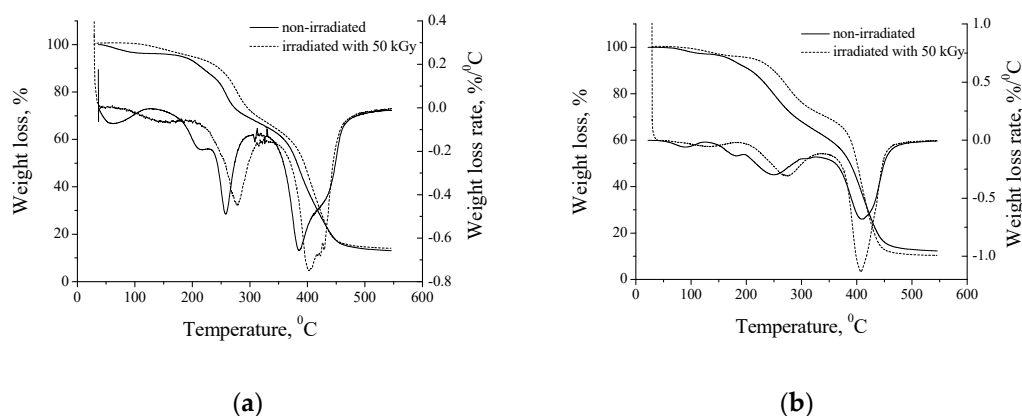


Figure 8. TG curves for (a) PAH18 and (b) PAH9 before and after irradiation.

4. Conclusions

Hydrogels having different equilibrium swelling degrees were prepared by γ -irradiation of either polymer or monomer aqueous solutions. When monomer solutions were used, higher absorbed doses were necessary for network formation, and the resulting gels were not macroscopically homogenous.

Polymers containing carboxyl and hydroxyl groups were prepared by radical solution polymerization of acrylic acid (AA) and 2-hydroxyethyl methacrylate (HEMA). The resulting polymers behaved like neutral polymers at pH 3, and had overlapping concentration below 1%. After irradiation, chemically crosslinked hydrogels were obtained with different structural parameters depending on adsorption doses.

FTIR and thermal behavior analysis for xerogels prepared by γ -irradiation of polymer aqueous solutions show that during irradiation mainly the functional groups are destroyed, while the polymer backbone remains unaffected.

Author Contributions: Conceptualization, T.S.; formal analysis, M.M., R.M.L., V.C., M.I. and T.S.; methodology, T.S., M.M. and V.C.; validation, T.S., M.M. and V.C.; writing—original draft preparation, T.S.; writing—review and editing, T.S. and M.M.; visualization, T.S.; supervision, T.S. All authors have read and agreed to the published version of the manuscript.

Funding: This research received no external funding.

Conflicts of Interest: The authors declare no conflict of interest.

References

- Lee, K.Y.; Mooney, D.J. Hydrogels for tissue engineering. *Chem. Rev.* **2001**, *101*, 1869–1879. [[CrossRef](#)] [[PubMed](#)]
- Khademhosseini, A.; Langer, R. Microengineered hydrogels for tissue engineering. *Biomaterials* **2007**, *28*, 5087–5092. [[CrossRef](#)] [[PubMed](#)]
- Jia, X.; Küick, K.L. Hybrid multicomponent hydrogels for tissue engineering. *Macromol. Biosci.* **2009**, *9*, 140–156. [[CrossRef](#)] [[PubMed](#)]
- Jabbari, E. Bioconjugation of hydrogels for tissue engineering. *Curr. Opin. Biotech.* **2011**, *22*, 655–660. [[CrossRef](#)]
- Censi, R.; Di Martino, P.; Vermonden, T.; Hennink, W.E. Hydrogels for protein delivery in tissue engineering. *J. Control. Release* **2012**, *161*, 680–692. [[CrossRef](#)] [[PubMed](#)]
- Hamidi, M.; Azadi, A.; Rafiei, P. Hydrogel nanoparticles in drug delivery. *Adv. Drug Deliv. Rev.* **2008**, *60*, 1638–1649. [[CrossRef](#)]
- Qin, Y.; Park, K. Environment-sensitive hydrogels for drug delivery. *Adv. Drug Deliv. Rev.* **2012**, *64*, 49–60.
- Buenger, D.; Topuz, F.; Groll, J. Hydrogels in sensing applications. *Prog. Polym. Sci.* **2012**, *37*, 1678–1719. [[CrossRef](#)]

9. Kotanen, C.N.; Tlili, C.; Guiseppi-Elie, A. Amperometric glucose biosensor based on electroconductive hydrogels. *Talanta* **2013**, *103*, 228–235. [[CrossRef](#)]
10. O'Grady, M.L.; Kuo, P.-L.; Parker, K.K. Optimization of electroactive hydrogel actuators. *Appl. Mater. Interfaces* **2010**, *2*, 343–346. [[CrossRef](#)]
11. Wang, E.; Desai, M.S.; Lee, S.-W. Light-controlled graphene-elastin composite hydrogel actuators. *Nano Lett.* **2013**, *13*, 2826–2830. [[CrossRef](#)] [[PubMed](#)]
12. Lee, B.P.; Konst, S. Novel hydrogel actuator inspired by reversible mussel adhesive protein chemistry. *Adv. Mater.* **2014**, *26*, 3415–3419. [[CrossRef](#)] [[PubMed](#)]
13. Lee, B.P.; Liu, M.-H.; Narkar, A.; Konst, S.; Wilharm, R. Modulating the movement of hydrogel actuator based on catechol-iron ion coordination chemistry. *Sens. Actuators B Chem.* **2015**, *206*, 456–462. [[CrossRef](#)]
14. Krogsgaard, M.; Behrens, M.A.; Pedersen, J.S.; Birkedal, H. Self-healing mussel-inspired multi-pH-responsive hydrogels. *Biomacromolecules* **2014**, *14*, 297–301. [[CrossRef](#)] [[PubMed](#)]
15. Zhang, Z.; Chen, L.; Deng, M.; Bai, Y.; Chen, X.; Jing, X. Biodegradable thermo- and pH-responsive hydrogels for oral drug delivery. *J. Polym. Sci. Pol. Chem.* **2011**, *49*, 2941–2951. [[CrossRef](#)]
16. Rodkate, N.; Rutnakornpituk, B.; Wichai, U.; Ross, G.; Rutnakornpituk, M. Smart carboxymethylchitosan hydrogels that have thermo- and pH-responsive properties. *J. Appl. Polym. Sci.* **2015**, *132*, 41505–41514. [[CrossRef](#)]
17. Li, L.; Xing, X.; Liu, Z. Triply-responsive (thermo/light/pH) copolymeric hydrogel of N-isopropylacrylamide with an azobenzene-containing monomer. *J. Appl. Polym. Sci.* **2012**, *124*, 1128–1136. [[CrossRef](#)]
18. Alzari, V.; Nuvoli, D.; Sanna, R.; Peponi, L.; Piccinini, M.; Bon, S.B.; Marceddu, S.; Valentini, L.; Kenny, J.M.; Mariani, A. Multistimuli-responsive hydrogels of poly(2-acrylamido-2-methyl-1-propanesulfonic acid) containing graphene. *Colloid Polym. Sci.* **2013**, *291*, 2681–2687. [[CrossRef](#)]
19. Park, S.K.; Guntur, S.R.; Lee, K.I.; Paeng, D.-G.; Choi, M.J. Reusable ultrasonic tissue mimicking hydrogels containing nonionic surface-active agents for visualizing thermal lesions. *IEEE Trans. Biomed. Eng.* **2010**, *57*, 194–202. [[CrossRef](#)]
20. Casciaro, S.; Conversano, F.; Musio, S.; Casciaro, E.; Sannino, A. Full experimental modelling of a liver tissue mimicking phantom for medical ultrasound studies employing different hydrogels. *J. Mater. Sci. Mater. Med.* **2009**, *20*, 983–989. [[CrossRef](#)]
21. Rodrigues, F.H.A.; Fajardo, A.R.; Pereira, A.G.B.; Ricardo, N.M.P.S.; Feitosa, J.P.A.; Muniz, E.C. Chitosan-graft-poly(acrylic acid)/rice husk ash based superabsorbent hydrogel composite: Preparation and characterization. *J. Polym. Res.* **2012**, *19*, 1–10. [[CrossRef](#)]
22. Kadlubowski, S.; Henke, A.; Ulanski, P.; Rosiak, J.M. Hydrogels of polyvinylpyrrolidone (PVP) and poly(acrylic acid) (PAA) synthesized by radiation-induced crosslinking of homopolymers. *Radiat. Phys. Chem.* **2010**, *79*, 261–266. [[CrossRef](#)]
23. Caykara, T.; Ozyurek, C.; Kantoglu, O. Investigation of thermal behavior poly(2-hydroxyethyl methacrylate-co-itaconic acid) networks. *J. Appl. Polym. Sci.* **2007**, *103*, 1602–1607. [[CrossRef](#)]
24. Vargun, E.; Usanmaz, A. Degradation of poly(2-hydroxyethyl methacrylate) obtained by radiation in aqueous solution. *J. Macromol. Sci. A Pure Appl. Chem.* **2010**, *47*, 882–891. [[CrossRef](#)]
25. Roberts, J.J.; Martens, P.J. Engineering Biosynthetic Cell Encapsulation Systems. In *Biosynthetic Polymers for Medical Applications*; Poole-Warren, L., Martens, P., Green, R., Eds.; Woodhead Publishing: Cambridge, UK, 2016.
26. Kadlubowski, S.; Henke, A.; Ulanski, P.; Rosiak, J.M.; Bromberg, L.; Hatton, T.A. Hydrogels of polyvinylpyrrolidone (PVP) and poly(acrylic acid) (PAA) synthesized by photoinduced crosslinking of homopolymers. *Polymer* **2007**, *48*, 4974–4981. [[CrossRef](#)]
27. Park, J.-S.; Kuang, J.; Gwon, H.-J.; Lim, Y.-M.; Jeong, S.-I.; Shin, Y.-M.; Khil, M.S.; Nho, Y.-C. Synthesis and characterization of zinc chloride containing poly(acrylic acid) hydrogel by gamma irradiation. *Radiat. Phys. Chem.* **2013**, *88*, 60–64. [[CrossRef](#)]
28. Bayramgil, N.P. Synthesis, characterization and drug release behavior of poly(1-vinyl 1,2,4-triazole) hydrogels prepared by gamma irradiation. *Colloid Surf. B* **2012**, *97*, 182–189. [[CrossRef](#)] [[PubMed](#)]
29. Abd El-Mohdy, H.L.; Mostafa, T.B. Synthesis of polyvinyl alcohol/malic acid hydrogels by electron beam irradiation for dye uptake. *J. Macromol. Sci. A* **2013**, *50*, 6–17. [[CrossRef](#)]

30. Ibrahim, S.M.; El Salmawi, K.M.; Zahran, A.H. Synthesis of crosslinked superabsorbent carboxymethyl cellulose/acrylamide hydrogels through electron-beam irradiation. *J. Appl. Polym. Sci.* **2007**, *104*, 2003–2008. [[CrossRef](#)]
31. Flory, P.J.; Rehner, J. Statistical mechanics of cross-linked polymer networks. II. Swelling. *J. Chem. Phys.* **1943**, *11*, 521–526. [[CrossRef](#)]
32. Adnadjevic, B.; Jovanovic, J. Hydrogel synthesis directed toward tissue engineering: Impact of reaction condition on structural parameters and macroscopic properties of xerogels. *Int. J. Polym. Sci.* **2011**. [[CrossRef](#)]
33. Richter, A.; Paschew, G.; Klatt, S.; Lienig, J.; Arndt, K.-F.; Adler, H.-J. Review on hydrogel-based sensors and microsensors. *Sensors* **2008**, *8*, 561–581. [[CrossRef](#)]
34. Fahimi, Z.; Parviz, M.; Orang, F.; Bonakdar, S. Synthesis of pH sensitive hydrogels based on poly vinyl alcohol and poly acrylic acid. *Iran. J. Pharm. Sci.* **2008**, *4*, 275–280.
35. Philippova, O.E.; Hourdet, D.; Audebert, R.; Khokhlov, A.R. pH-responsive gels of hydrophobically modified poly(acrylic acid). *Macromolecules* **1997**, *30*, 8278–8285. [[CrossRef](#)]
36. Mittal, K.L. *Acid-Base Interactions: Relevance to Adhesion Science and Technology*; VSP: Utrecht, The Netherlands, 2000.
37. Choi, J.; Rubner, M.F. Influence of the degree of ionization on weak polyelectrolyte multilayer assembly. *Macromolecules* **2005**, *38*, 116–124. [[CrossRef](#)]
38. Rainaldi, I.; Cristallini, C.; Ciardelli, G.; Giusti, P. Copolymerization of acrylic acid and 2-hydroxyethyl methacrylate onto poly(*N*-vinylpyrrolidone): Template influence on comonomer reactivity. *Macromol. Chem. Phys.* **2000**, *201*, 2424–2431. [[CrossRef](#)]
39. Available online: <http://polymerdatabase.com/polymer%20chemistry/Qetable.html>. (accessed on 13 July 2020).
40. Colby, R.H. Structure and linear viscoelasticity of flexible polymer solutions: Comparison of polyelectrolyte and neutral polymer solutions. *Rheol. Acta* **2010**, *49*, 425–442. [[CrossRef](#)]
41. Wolf, B.A. Polyelectrolytes revisited: Determination of intrinsic viscosities. *Macromol. Rapid Commun.* **2007**, *28*, 164–170. [[CrossRef](#)]
42. Rosiak, J.M.; Ulanski, P. Synthesis of hydrogels by irradiation of polymers in aqueous solution. *Radiat. Phys. Chem.* **1999**, *55*, 139–151. [[CrossRef](#)]
43. Mohamed, K.; Gerasimov, T.G.; Moussy, F.; Harmon, J.P. A broad spectrum analysis of the dielectric properties of poly(2-hydroxyethyl methacrylate). *Polymer* **2005**, *46*, 3847–3855. [[CrossRef](#)]
44. Kabanov, V.P.; Dubnitskaya, V.A.; Khar'kov, S.N. Thermal properties of polyacrylic acid. *Poly. Sci. USSR* **1975**, *17*, 1848–1855. [[CrossRef](#)]
45. Fyfe, C.A.; McKinnon, M.S. Investigation of the thermal degradation of poly(acrylic acid) by high-resolution ¹³C CP MAS/NMR spectroscopy. *Macromolecules* **1986**, *19*, 1909–1912. [[CrossRef](#)]
46. Dubinsky, S.; Grader, G.S.; Shter, G.E.; Silverstein, M.S. Thermal degradation of poly(acrylic acid) containing copper nitrate. *Polym. Degrad. Stab.* **2004**, *86*, 171–178. [[CrossRef](#)]
47. Moharram, M.A.; Khafagi, M.G. Thermal behavior of poly(acrylic acid)-poly(vinyl pyrrolidone) and poly(acrylic acid)-metal-poly(vinyl pyrrolidone) complexes. *J. Appl. Polym. Sci.* **2006**, *102*, 4049–4057. [[CrossRef](#)]
48. Demirelli, K.; Coskun, M.; Kaya, E. A detailed study of thermal degradation of poly(2-hydroxyethyl methacrylate). *Polym. Degrad. Stab.* **2001**, *72*, 75–80. [[CrossRef](#)]

